THE BELL SYSTEM TECHNICAL JOURNAL
Vol. 50, No. 9, November, 1971
Printed in U.S.A.

An Experimental MM-Wave Path Length Modulator

By W. J. CLEMETSON, N. D. KENYON, K. KUROKAWA, B. OWEN, and W. O. SCHLOSSER

(Manuscript received June 3, 1971)

A modulation scheme in which the transmission path length of the mm-wave signal is digitally modulated by means of a PIN diode switch has been proposed for the waveguide transmission system. To demonstrate the feasibility of this proposal, a complete transmitter has been developed in the 50 ~ 60-GHz range, consisting of an IMPATT oscillator, circulator, PIN diode switch, and its driver circuit. The model can handle signals at 300 Mb/s and deliver 100 mW of modulated power at the output. This paper describes the design considerations of each component in detail, together with the experimental results.

I. INTRODUCTION

The availability of mm-wave silicon IMPATT diodes[1] with several hundred milliwatts of output power makes practical the construction of reliable all-solid-state mm-wave communication systems. Several candidate schemes have been proposed.[2-9] They can be divided into two broad categories, depending on whether the modulation is achieved within the oscillator circuit or separately.

The varactor tuned oscillator and the direct deviator are examples of achieving the modulation within the oscillator.

A method by which the path length of the mm-wave is modulated by a PIN diode switch is described in this paper and is an example of externally modulating a fixed-frequency oscillator. It represents the best compromise with respect to the required driving power, insertion loss, speed, and power handling capability at mm-wave frequencies. In particular, we have concentrated on two-level Path Length Switched Differentially Coherent Phase Shift Keying, in short, PLS-DCPSK. This paper describes the development of an experimental mm-wave PLS-DCPSK transmitter in the 50 ~ 60-GHz range. The model is

capable of handling signals at a rate of 300 Mb/s and delivers 100 mW of modulated power at the output port.

II. PLS-DCPSK

The principle of PLS-DCPSK is best illustrated by referring to Fig. 1. The mm-wave power from a fixed oscillator is fed into a PIN diode switch through a circulator. When the switch is closed, the wave is reflected at the diode position, and when it is open, the wave is reflected at the short circuit a quarter-wavelength behind the diode. The phase of the transmitted mm-wave, therefore, changes by 180 degrees whenever the switch changes its state[10,11] corresponding to incoming signal "1" as illustrated in Fig. 2. At the receiver, the RF phases one time interval (3.33 ns for 300-megabaud signals) apart are compared by means of a delay line and hybrid circuits. When the phase difference is 180 degrees the detector output becomes "1" and when there is no phase difference, the output becomes "0." Thus, the receiver output becomes a duplicate of the original signal. In addition to the phase switching, the amplitude can be modulated to send, for example, a timing signal, if so desired.

The two principal advantages of this modulation scheme are separation of generation and modulation functions, and digital operation of the modulator. Because of the first feature, the oscillator and modulator can be optimized independently. No compromises are required between conflicting factors in the oscillator design, such as low Q for modulation sensitivity and high Q for low noise and frequency stability. The oscillation frequency can be made very stable and the oscillation noise low by using a high Q stable oscillator circuit. Should a more efficient

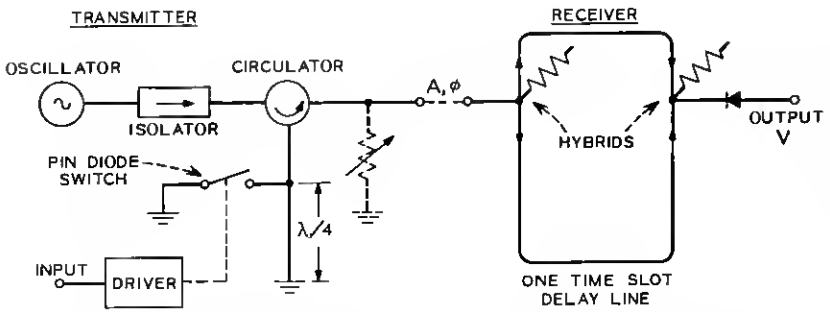

Fig. 1—A schematic diagram of PLS-DCPSK transmitter and receiver.

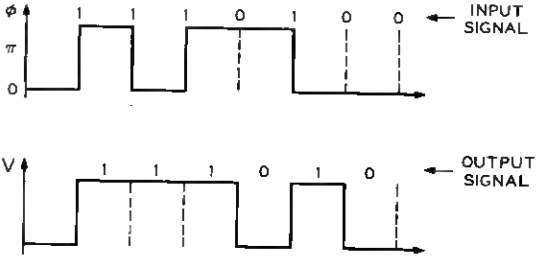

Fig. 2—The RF phase φ and the detector output V in relation with the input and output signals.

oscillator (with the same output power) be developed in tbe future, the original oscillator can be replaced by the new one without redesigning the modulator, since it is independent of the oscillator tuning characteristics. Because of the digital operation, the characteristics of the modulator are not sensitive to small changes in the environmental temperature or in the bias voltage. The modulator has additional flexibility: by adding a 90-degree phase switch, we can extend the two-level operation of PLS-DCPSK to four-level operation, increasing the information rate by a factor of two.

On the other hand, the path length modulator system needs two semiconductor devices: an IMPATT diode and a PIN diode, plus a circulator or a 3-dB coupler. In addition, we have to accept an insertion loss due to the modulator, which in the 50 $\sim$ 60-GHz range is of the order of 1 dB.

In the following sections, we discuss, in turn, the oscillator, the circulator, the PIN diode, and the driver circuit.

III. THE OSCILLATOR

It is possible to build mm-wave IMPATT oscillators witb sufficient output power for mm-wave communication systems by providing several tuning elements and adjusting them by trial and error. However, frequency jumps and sudden increases of noise being common during the circuit and bias adjustment, it is difficult to predict the performance of such oscillators or to establish a systematic tuning procedure. These complications occur when the impedance locus $Z(\omega)$ intersects the device line $\bar{Z}(A)$ more than once, indicating more than one possible mode of oscillation. [$Z(\omega)$ is the circuit impedance presented to the device and $\bar{Z}(A)$ is the negative of the device impedance as a function of

the RF current amplitude A.] For a stable oscillator circuit with predictable performance,[12] the impedance locus must intersect the device line once and only once over the active frequency range of the device. Attempts to realize such an oscillator circuit with lossless elements have not succeeded, and hence the lossless restriction is relaxed.

We will next describe the evolution of an equivalent circuit which gives a suitable impedance locus.

3.1 *Equivalent Circuit and Hardware*

In the design of oscillator circuits, a dc bias has to be applied to the diode. The bias connection inevitably forms a part of the RF circuit, so it is desirable to select a geometric form whose microwave transmission properties are well known. This leads one to choose a uniform two-conductor transmission line shown in Fig. 3a. In this form, the open-circuit to the right will cause an undesired frequency dependent reflection; the only way to prevent this is to add a matched termination shown in Fig. 3b as Z_0. This approach is legitimate only if the useful load, which may be thought of as coupled in some way to the transmission line, presents a series resistance much higher than the characteristic impedance of the transmission line. This situation is depicted in Fig. 3c. A small fraction of the output power may be wasted in the bias line termination, but in return we obtain a truly single-tuned stable circuit free from multiple-intersections between the impedance locus and the device line.[13–15] A similar approach was first used by E. T. Harkless.[16]

Since we require operation only at a single frequency and need a high

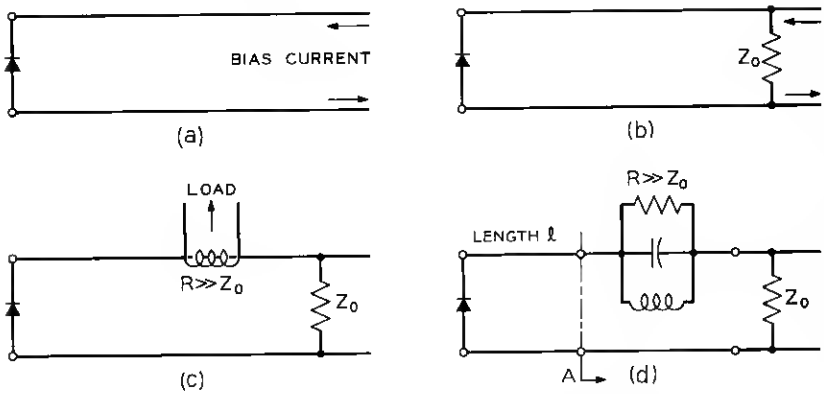

Fig. 3—Step-by-step construction of the equivalent circuit.

resistance at the operation frequency, the natural approach is to make the load in Fig. 3c look like a parallel resonant circuit as shown in Fig. 3d. The combined impedance, load and termination, has an impedance locus like the solid circle on the Smith chart of Fig. 4; at resonance the resistance of the load circuit is much greater than Z_0 while away from resonance only the termination is effective. On this chart, we have also shown the device line and the optimum operating point. In order to reach this point at resonance, we first change the diameter of the resonance circle, in this case to the dotted one at the right. Secondly, we interpose a length l of the uniform transmission line, displacing the circle by an angle $\theta = 4\pi l/\lambda$ (λ = wavelength) clockwise about the center of the chart to the required point. The clockwise rotation is easy to understand. To explain the change of circle diameter, let us expand the parallel resonant load in a more realistic form. Referring to Fig. 5, it takes a form of a high Q microwave cavity, coupled by some coupling K_2 into the main waveguide, and itself coupled at K_1 onto the transmission line. The external Q of the oscillator will be almost exactly the loaded Q of this cavity. The loaded Q must be much smaller than the unloaded Q, in order to minimize the power wasted in the cavity and to maximize the circuit efficiency. The external loading is adjusted by K_2 , leaving K_1 to control the diameter of the impedance circle. As K_1 is tightened, the diameter of the circle increases; thus K_1 is in the nature of a power optimizing element. However, it may happen that K_1 has some natural maximum and we may still not have enlarged the circle diameter enough to reach the optimum operating point. Then, it is necessary to move the optimum operating point towards the center of the chart, which can be accom-

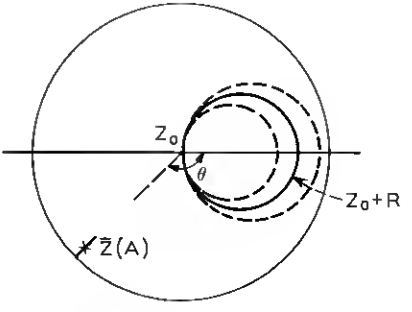

Fig. 4—Impendance locus looking from reference plane A in Fig. 3d and device line. The optimum operating point is indicated by x.

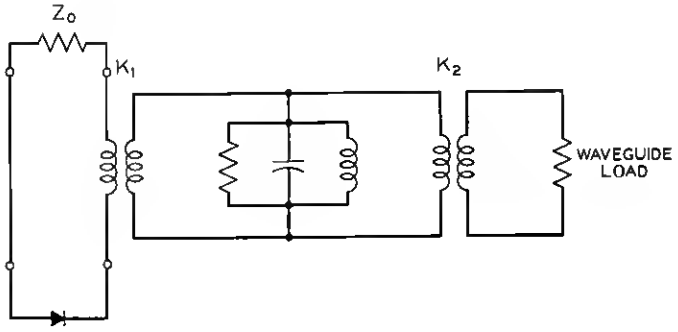

Fig. 5—Oscillator equivalent circuit.

plished by inserting a transformer close to the diode in such a way as to improve its effective resistance level by a factor of two or three. It was necessary to do this for the mm-wave diodes.

Figure 6 shows a physical realization of the equivalent circuit. The transmission line is shown as a terminated coaxial line of about 50 Ω impedance with a place for the IMPATT diode; it passes through a half-wavelength rectangular waveguide cavity which is coupled by an iris to the output waveguide, K_2 . The coupling K_1 is adjustable over a limited range by a movable short-circuit placed immediately behind the center conductor. Figure 7 is the actual circuit used at 57 GHz. It has some features not shown in Fig. 6: the transformer previously mentioned is inserted immediately above the diode, and the length l of transmission line is adjusted by means of spacers, so shaped that mechanical pressure gives good electrical contact to avoid losses. The quartz rod serves to compensate the cavity resonance for changes in temperature and, independently, as a fine frequency control.

The rectangular waveguide cavity resonates in the TE_{101} mode. The cavity will also resonate in higher modes such as TE_{201} , TE_{102} , etc. However, at these resonant frequencies, the impedance locus $Z(\omega)$ will be located so far from the device line that no multiple intersections will occur. This is because the rotation $\theta = 4\pi l/\lambda$ of the resonant impedance is now too large (small values of λ) and overshoots the position of the device line at the corresponding frequencies. Also, the coupling coefficients K_1 and K_2 for most higher modes do not lead to intersection of the circuit impedance with the device line. At the higher resonant frequencies the diode will cease to show a negative resistance.

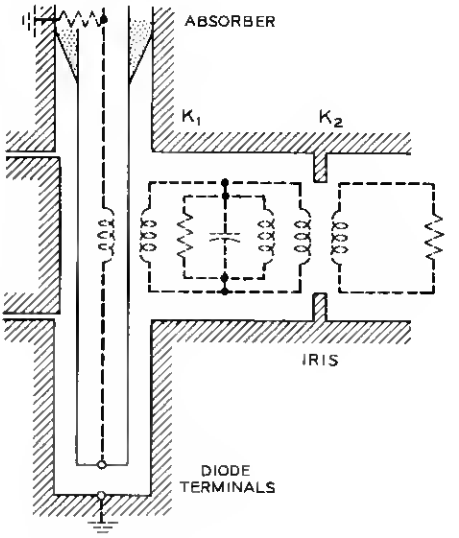

Fig. 6—Hardware around the equivalent circuit of Fig. 5.

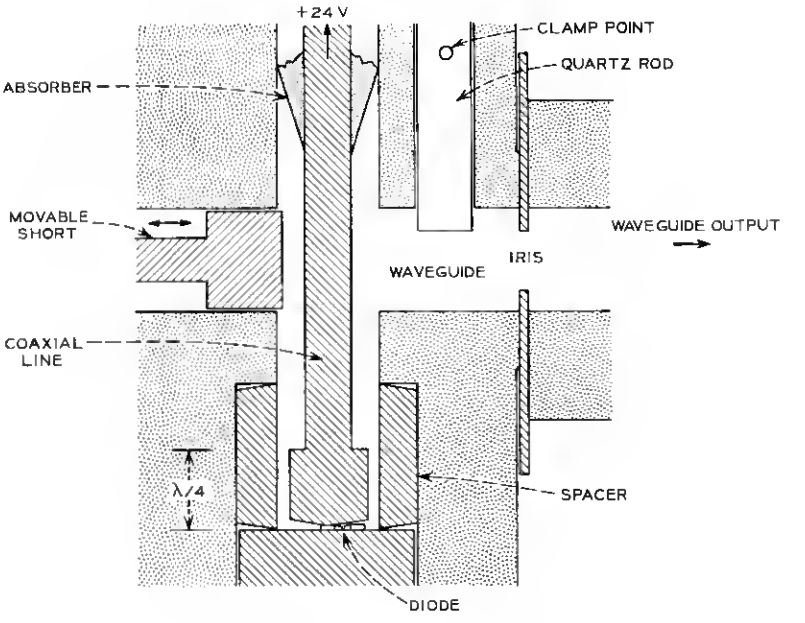

Fig. 7—Oscillator structure.

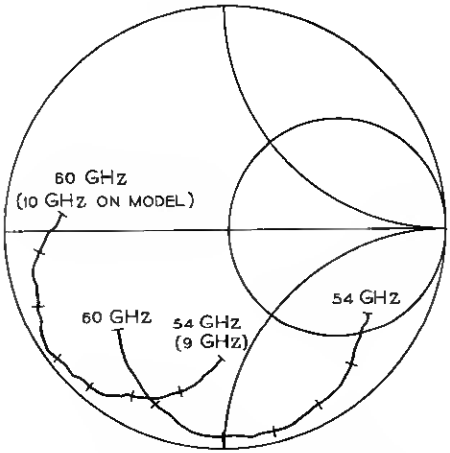

Fig. 8—Impedance seen at diode position on X-band model for two values of the transmission line length.

3.2 *Experimental Results*

In order to check that the mechanical configuration shown in Fig. 6 gives the desired impedance locus, a scale model was built in X-band and a network analyzer was used to measure the impedance seen from the diode terminals. The examples in Fig. 8 show that we obtained the smooth single-tuned behavior desired. Figure 9 shows how the mm-wave oscillator output power and frequency varied with the position of the sliding short; there is a power optimum at about 0.3 mm, and the frequency actually rises as the short is withdrawn. The more

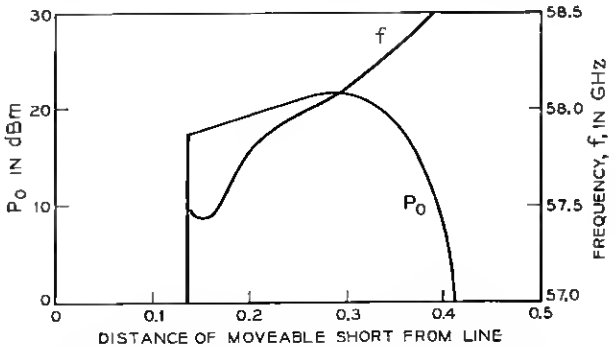

Fig. 9—Output power and frequency vs short position.

extensive impedance measurements on the X-band model show that such behavior is to be expected.

Results from a variety of mm-wave diodes are listed in Table I. The bias current was adjusted to produce 125 $\sim$ 130 mW. The diode temperature was measured by momentarily pulsing down the bias voltage and measuring the breakdown voltage, which is a function of the diode temperature. The efficiencies are somewhat low because the diodes were being operated well below the current density needed for maximum efficiency. The external Q's were of the order of 100. Should a higher external Q be desired, further improvement of the unloaded Q of the cavity would be necessary. However, the performance of these oscillators was already quite satisfactory for this application.

IV. THE CIRCULATOR

A symmetrical three-port junction circulates when the reflection coefficients of its three characteristic excitations are of the same magnitude and are mutually phase displaced by $2\pi/3$ radians. These excitations are the eigenvectors of the junction scattering matrix, and the reflection coefficients are the corresponding eigenvalues.[17] One excitation has its components in phase in all three ports. The other two have their components displaced by $2\pi/3$ radians from port to port, and rotate in opposite directions. The reflection coefficients are determined by the internal modes associated with these excitations and by their interaction with the enclosed ferrite.

In the compact turnstile circulator,[18] dielectric spacers are used to couple the rotating excitations to circularly polarized modes which propagate along the ferrite axis. These modes experience different permeabilities when the ferrite is magnetized, and the phases of their reflection coefficients are essentially determined by the ferrite length

TABLE I—TYPICAL CHARACTERISTICS OF IMPATT OSCILLATOR

Diode No.	Power mW	Efficiency %	Current mA	Temp. °C	$\Delta f/\Delta T$ kHz/°C	Freq. GHz
1	125	3.8	150	175	—	—
2	125	3.7	150	175	—	—
3	125	3.3	165	230	+200	57.4
4	125	4.1	142	210	−100	56.4
5	125	3.9	142	210	—	57.4
6	130	5.3	100	225	−600†	57.4

† Insufficient quartz clamping length.

and applied magnetic field. They are affected only slightly by the ferrite diameter. The in-phase excitation, on the other hand, cannot couple to an axially propagating mode. It sees the ferrite simply as a dielectric resonator, and the phase of its reflection coefficient is largely determined by the ferrite diameter. By adjusting the ferrite length, diameter, and applied magnetic field, the three reflection coefficients may be phase displaced from one another by $2\pi/3$ radians and circulator operation is achieved.

A cross section of the circulator developed for the path length modulator is shown in Fig. 10. The ferrite was recessed into the metal junction both to provide a secure mount and to assure its symmetrical disposition. An air gap was used to provide the dielectric discontinuity required to couple the rotating excitations to axially propagating modes. The use of air simplified the coupling adjustment in development and avoided any dependence on dielectric properties such as loss and dielectric constant. A quarter-wave transformer was used as an aid in matching into the junction.

The ferrite chosen was a nickel-zinc material with a 5000-gauss saturation magnetization. The ferrite diameter and length were approximately 3/4 wavelengths and 5/4 wavelengths respectively, as measured in the infinite ferrite medium. The circulator could in principle operate with any odd number of quarter wavelengths for the ferrite length. In this case the rectangular waveguide height dictated the choice of 5/4 wavelengths. A biasing field of approximately 600 gauss was required.

The measured characteristics are shown in Fig. 11. Isolation of 20 dB was achieved over a 4-percent bandwidth, and the insertion loss was less than 0.25 dB across this band.

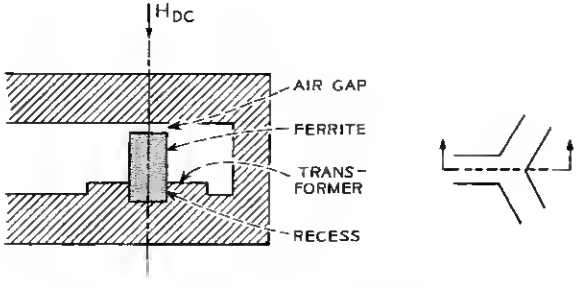

Fig. 10—Circulator cross section.

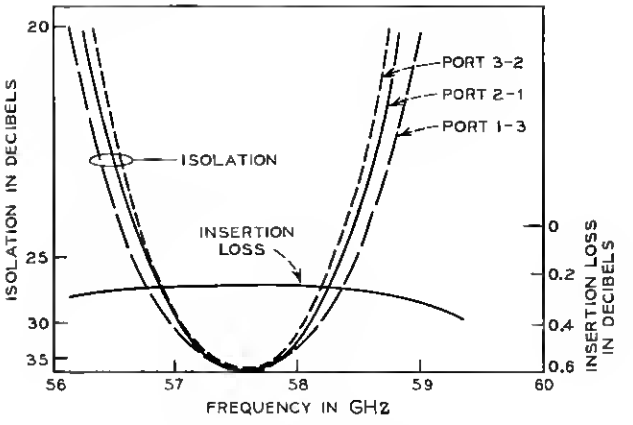

Fig. 11—Circulator characteristics.

V. THE PIN DIODE

PIN diodes can support RF current substantially greater than the forward bias current. In the reverse bias state, the capacitance per unit area of PIN diodes is relatively small and independent of the bias voltage. This means that the impedance level of the switch circuit can be made relatively high (for a specified power handling capability) and the switch characteristic is approximately independent of the bias voltage. Neither Schottky barrier diodes nor p-n junction diodes have these desirable features.

Schottky barrier diodes will probably provide the fastest switching action among available semiconductor devices. However, when a switching time of the order of a half ns is acceptable, PIN diodes are superior with respect to power handling capability, insertion loss, impedance level, and harmonic content. The use of a transferred-electron diode[19,20] or avalanche diode as a switching element cannot be justified in our case because of the high driving power required; for these devices, high bias current and high voltage must be applied simultaneously.

We now discuss the design of a PIN diode for the mm-wave switch application.[21]

5.1 *Design*

The design of the PIN diode is so intimately related to both the driver and the mm-wave circuit that the three must be jointly designed.

The i layer thickness of the diode is primarily determined by the available pulse voltage from the driver. A pulse amplitude of the order of 10 V is a reasonable target for any transistorized driver for mm-wave repeater applications. Then the RF peak voltage one can apply to the reverse biased PIN diode without introducing too much loss is also approximately 10 V; so the breakdown voltage must be larger than 20 V to realize the full advantage of the available driver pulse voltage. Taking into account possible field nonuniformity in the i layer, especially during the switching transient, a breakdown voltage of 40 V was considered to be a good objective. Since the breakdown field is 2×10^5 V/cm in silicon, 40 V breakdown voltage requires a 2 μ thick i layer.

The cross-sectional area of the diode is determined by the practical impedance level of the mm-wave circuit. In order to get 180-degree phase differences with equal insertion losses in the two switching states, the real and imaginary parts of the mm-wave circuit impedance presented to the diode must each be approximately one-half of the impedance of the i layer capacitance, assuming that the series resistance stays the same in the two states [see equation (5) in Appendix]. Suppose that we can present approximately $(50 + j50)\Omega$ to the diode without introducing too much loss, then the desired $1/\omega C$ is 100 Ω or C is approximately 0.026 pF at 60 GHz. With a 2 μm thick i layer, the diode diameter is calculated to be of the order of 25 μm.

Now, we have to check the power handling capability of the 180-degree phase switch. A simple equivalent circuit shows that, if the RF voltage swing across the i layer is limited to ± 10 V as previously assumed, the switch can handle about 125 mW provided that the forward bias state can support sufficient RF current (see Appendix). In the forward bias state the diode should be almost short circuited. The peak RF current under this condition is calculated to be approximately 100 mA. This value of RF current can be used to determine the forward bias current and is considered next.

Suppose that the carrier (electron) velocity is 10^6 cm/s (about one-tenth of the saturation velocity), then the transit time for the 2 μm thick layer becomes 0.2 ns. The required forward bias current is equal to the peak RF current multiplied by the ratio of the electron transit time to lifetime (neglecting the contribution of holes to the RF current). If we assume the lifetime to be about 10 ns, the forward bias current is calculated to be 2 mA which is a quite reasonable value for a transistorized driver. However, before fixing the bias current, it is necessary to check the RF series resistance of the i layer. If the electron mobility in the i layer is conservatively assumed to be 1000

$cm^2/V\text{-}s$,† the RF field corresponding to a velocity of 10^6 cm/s is 1000 V/cm; thus, the RF voltage across the i layer is 0.2 V, and the RF resistance of the i layer under the forward bias condition is 2 Ω, which is rather high. To reduce the series resistance, the bias current has to be increased. In fact, bias current up to 10 mA is used depending on the wafer. The corresponding RF series resistance is about 0.4 Ω.

Finally, we have to check the switching times. The forward switching time is limited by the i layer thickness divided by the saturation velocity. This is about 20 ps. After the carriers reach the other sides of the i layer, it takes a relatively long time (of the order of lifetime) before steady state is reached. However, during this period the RF impedance does not change appreciably and for all practical purposes the forward switching time of the PIN diode is negligible compared to the time constant of transistorized drivers. The reverse switching time is determined by how quickly the charge stored in the i layer can be removed. Since the stored charge is given by the forward bias current multiplied by the lifetime of the carriers, the reverse switching time is given by the product of the lifetime and ratio of the forward bias current to the driving current.[22] If we assume 10 V pulse height and 20 Ω output impedance for the driver, the initial driving current becomes 500 mA, so that a reverse switching time of the order of a half nanosecond should be achievable.

In the above calculation, it is assumed that the diode works as a PIN diode rather than a p-n junction diode. The validity of this assumption may be questioned because of the extremely thin i layer. Fortunately, the forward dc characteristic, the backward capacitance characteristic, and the RF behavior all indicate that most of the diodes are working as PIN diodes in the bias range mentioned above.

It is assumed that the RF current distribution is uniform over the entire cross section. Since the resistivity to give 0.4 Ω RF series resistance with the given dimensions is calculated to be 0.01 Ω-cm and the corresponding skin depth approximately 20 μm, the uniform current assumption seems to be appropriate.

Finally, the above calculation is based on an assumed lifetime of 10 ns. If the lifetime is longer, the forward bias current should be decreased to get similar switching characteristics. If it is shorter, the bias current should be increased. In fact, our experiments indicate that the lifetime varies over a wide range from one wafer to another

† No particular significance should be attached to this value used for the rough estimate of the RF resistance.

and the bias current is best determined experimentally after diodes are fabricated.

5.2 *Fabrication*

In the preceding discussion of PIN diode design, we have neglected the detrimental effects of contact resistance, substrate resistance, and resistance in doping tails. The substrate resistance is kept low by minimizing its thickness, and the contact resistance by optimizing metallization and bonding techniques. The doping tails occur in practice at both ends of the i layer, where ideally we would prefer abrupt transitions to the p and n regions. In the reverse biased state, these doping tails are not completely depleted and present a relatively high resistance in series with the i layer capacitance. To reduce this effect, the fabrication of the diode should be such that the doping tails are short compared to the total thickness of the i layer which is 2 μm in our case.

The actual fabrication of diodes starts with the expitaxial growth of the 2 μm thick i layer on an arsenic-doped silicon substrate with resistivity about 0.001 Ω-cm. The transport reaction responsible for the expitaxial growth is hydrogen reduction of $SiCl_4$. Special care must be taken to use a high-resistivity silicon susceptor to achieve a relatively high resistivity of the order of 10 Ω-cm in the i layer. The substrate is kept at 1170°C. The typical doping tail obtained is 0.4 $\sim$ 0.6 μm long, which seems to be acceptable for switches at least in the 50 $\sim$ 60-GHz range.

Boron is then diffused to a depth of 0.25 μm by placing the slice in a furnace at 875°C for 60 minutes. The relatively low temperature and short time are used both to prevent further out-diffusion from the highly doped substrate into the i layer and to make the doping profile sharp on the p side.

The substrate is then lapped to a thickness of approximately 10 μm. The stresses developed by lapping are removed by a light etch. The slice must then be thoroughly cleaned before metallization. Extreme care must be exercised in this step; otherwise, good metal adherence will not be achieved in the subsequent process. After cleaning, 200 Å of titanium and 1000 Å of gold are evaporated on both sides of the slice. The gold is then plated up to a thickness of 5 μm. A photoresist pattern of approximately 70-μm diameter dots is applied and the slice is etched apart into diode chips.

Each diode is then thermocompression bonded onto a burnished,

gold-plated copper stud 3.2 mm in diameter, using a pressure of 700 Kg/cm^2 at about 330°C. These parameters have been carefully optimized by experiment. Two quartz standoffs, metallized on the top and bottom surfaces, are also bonded to the stud as close as possible to the diode. These standoffs are connected to the diode with a short thin gold ribbon. The diode is then etched to the final diameter and baked in a nitrogen atmosphere to dry it thoroughly. This completes the diode fabrication. Figure 12 shows an electron microscope picture of a finished diode. The silicon has been etched back to an appropriate diameter and appears as the black column at the center. The discs at both ends of the column are thin gold dots. To distinguish the top and bottom of the diode, the bottom disc is made squarish. The gold ribbon is bonded on the upper circular disc.

5.3 *The Diode Mount*

As we mentioned earlier, the 180-degree phase shift is obtained when the waveguide impedance, transformed to a value determined by the diode impedance, is presented to the diode. Since the external circuit

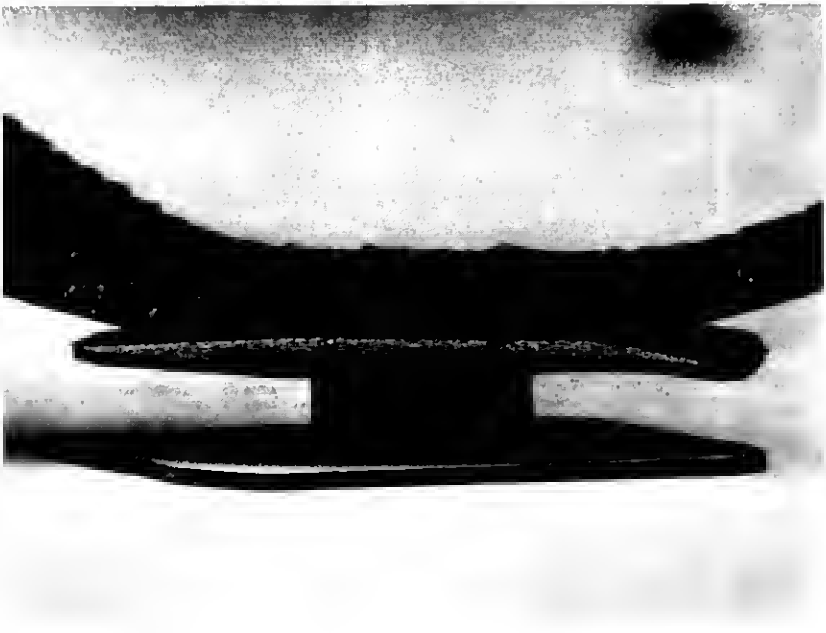

Fig. 12—Electron microscope picture of a PIN diode.

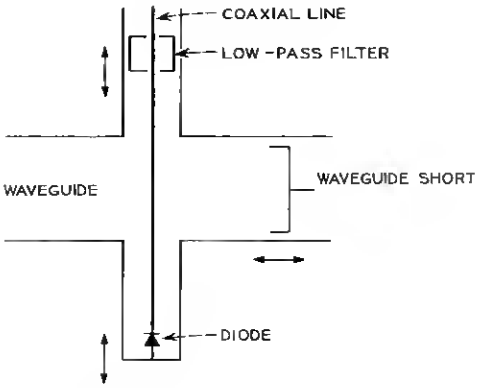

Fig. 13—Schematic diagram of the diode mount.

is connected to the diode at the top of the quartz standoffs and it is not obvious what kind of transformation is performed by that part of the circuit (consisting of the gold ribbon and the standoffs), the diode mount is designed in such a way as to permit all possible impedance transformations. The diode is mounted at one end of a coaxial line cross coupled to a short-circuited waveguide as illustrated in Fig. 13. The other end of the coaxial line is terminated by a low-pass filter through which the bias voltage is applied to the diode. Assuming that both the filter position and the waveguide short are adjustable, let us consider the impedance looking into the coaxial line from the diode position. An equivalent circuit of the coaxial-to-waveguide junction is shown in Fig. 14. The coaxial line is in series with the waveguide

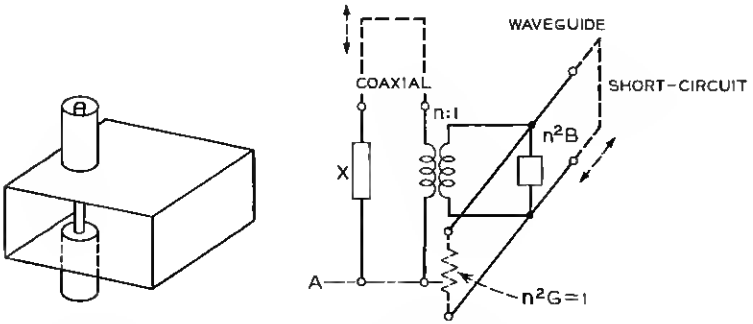

Fig. 14—Equivalent circuit of coaxial-to-waveguide symmetrical junctions.

which is in turn a parallel connection of the characteristic admittance $Y_0 = G$ and some susceptance due to B and the short-circuited waveguide. From this equivalent circuit, the possible range of impedance which is realizable at reference plane A by adjusting the waveguide short and the coaxial filter position is given by the shaded area in the Smith chart of Fig. 15. If we avoid the coaxial position too close to the waveguide sidewall, G becomes less than one. Thus, any impedance on the Smith chart becomes realizable at the diode position (which is also adjustable along the coaxial line).

A cross section of the actual diode mount is shown in Fig. 16. The tuning spacers are replaceable and the retaining screws secure good electrical contact. The coaxial line is located about a quarter of the waveguide width off the center in order to reduce B and X in Fig. 14 so that the circuit adjustment becomes less critical.

5.4 *Diode Characteristics*

The same type of diode mount is used for the diode $\hat{Q}$ measurement. The quality factor $\hat{Q}$ of switching diodes is defined by[23]

$$\hat{Q} = \frac{|Z_1 - Z_2|}{\sqrt{r_1 r_2}}$$

where Z_1 and Z_2 are the diode impedances under the reverse and forward bias conditions to be used in the switch (+10 mA forward and −10 V

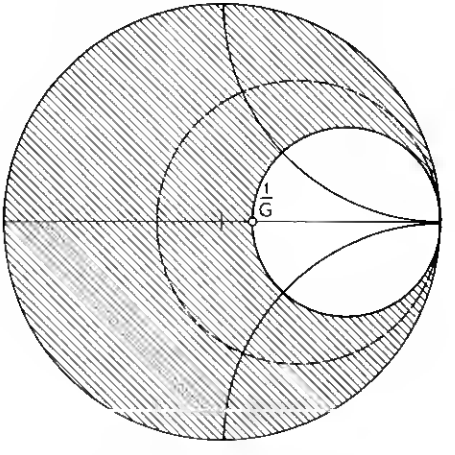

Fig. 15—Possible range of impedance at reference A in Fig. 14 (solid line $G < 1$, dotted line $G > 1$).

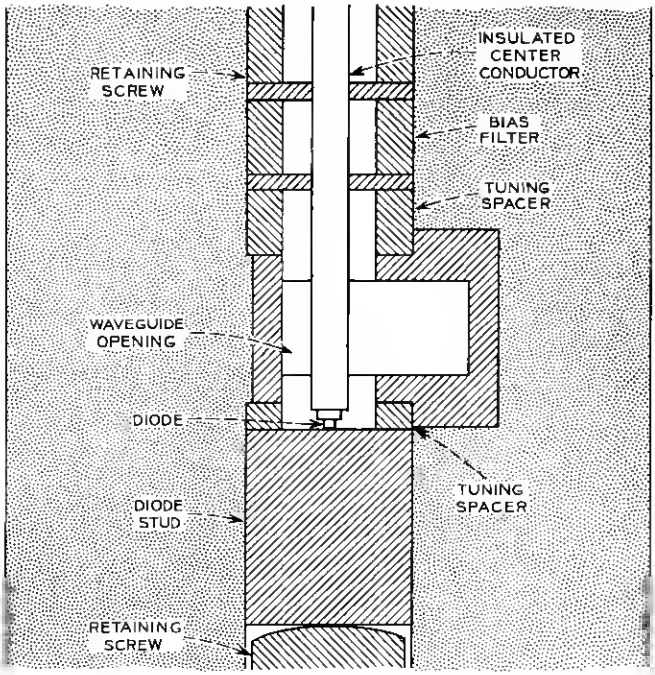

Fig. 16—PIN diode mount for 180-degree phase switch.

reverse in our case) and r_1 and r_2 are the real parts of Z_1 and Z_2 . The best PIN diode yet tested showed $\hat{Q}$ to be about 40 at 57 GHz, corresponding to an insertion loss of about 0.4 dB for a 180-degree phase shifter. In addition to $\hat{Q}$, we usually measure the breakdown voltage at a reverse current of 0.1 μA, the packaged capacitance at -10 V, and the dc incremental resistance at 10 mA and 100 mA of forward bias current. Table II shows typical results. The correlation between $\hat{Q}$ and the incremental resistance is fair.

VI. THE DRIVER

A high-speed driver circuit is needed to activate the PIN diode switch. It is also necessary to convert the input binary information into a differential binary signal before driving the PIN diode as is evident from Fig. 2. A driver circuit which incorporates a step-recovery diode pulse generator, a high-speed flip-flop, and a high-speed pulse amplifier was developed. A detailed description of the circuit and of

TABLE II—TYPICAL CHARACTERISTICS OF PIN DIODE

Diode No.	Q	BV (V)	Packaged Capacitance (pF)	Forward Resistance (Ω)	
				at 10 mA	at 100 mA
1	35	42	0.087	3.3	0.3
2	25	30	0.098	11.8	1.3
3	20	42	0.104	6.6	1.0
4	30	42	0.086	4.2	0.9
5	40	42	0.100	5.0	0.35

experimental results obtained with the complete path length modulator follows.

6.1 *Circuit Description*

A block diagram of the driver circuit is shown in Fig. 17. The high-speed flip-flop circuit requires that the trigger pulse be narrow ($\cong$1.2 ns). The step-recovery diode pulse generator provides this narrow pulse to ensure reliable triggering of the flip-flop. The flip-flop converts the binary information into a differential binary signal. This signal is then amplified to drive the PIN diode switch which shifts the phase of the RF carrier by 180 degrees.

The step-recovery diode pulse generator and the high-speed flip-flop were originally designed by D. Koehler[24] and modified by T. O'Shea and W. E. Ballentine. The technique they used to obtain the high-speed operation of the flip-flop was the utilization of pulse routing which provides a sufficiently high-current trigger source. Also, an emitter follower was used in the collector-to-base feedback loop of the flip-flop to provide a base current spike necessary for fast switching without overloading the collector circuit.

The complete driver schematic is shown in Fig. 18. The binary input is applied to the pulse generator which consists of a charge-storage step-recovery diode D_1 and a Schottky barrier diode D_2 . Diode D_2 provides a forward-current charging path for the step-recovery

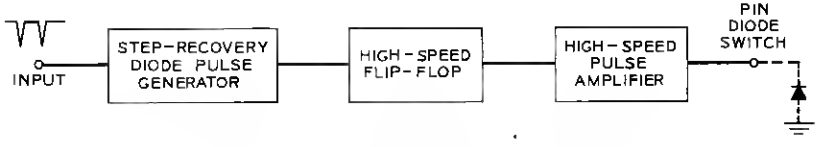

Fig. 17—Block diagram of the driver circuit.

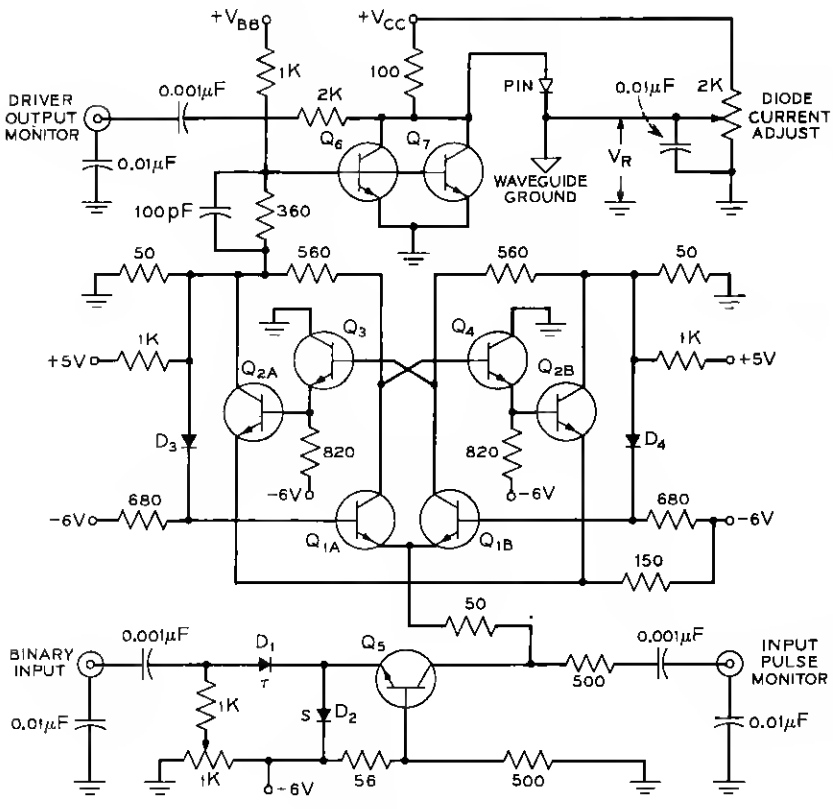

Fig. 18—Schematic diagram of the driver circuit.

diode. A negative input pulse will cut D_2 off and remove the charge stored in D_1 to obtain the step-recovery effect. The common base amplifier (Q_5) amplifies the resulting fast pulse. This provides a trigger pulse of about 1.2 ns width and 10 mA amplitude, which drives the steering transistors (Q_{1A} and Q_{1B}). The state of the flip-flop is fed back to the steering transistors by level shifting diodes D_3 and D_4. The trigger pulse is then routed to the emitter followers (Q_3 or Q_4) which provide the base current spike to switch the flip-flop transistors (Q_{2A} or Q_{2B}). The flip-flop output is then applied to the pulse amplifiers (Q_6 and Q_7).

In order to drive the PIN diode from forward conduction to reverse bias, the driver circuit is floated by a voltage corresponding to the diode reverse voltage (V_R). The output drive transistor operates

basically as a switch. When the flip-flop output is zero, the transistor is forward-biased by V_{BB} and the reverse voltage V_R is applied to the PIN diode. When the flip-flop output is -1 V, this provides a negative bias which turns off the drive transistor and the PIN diode is forward-biased. The forward current is determined by the difference between V_{CC} and V_R .

The output drive amplifier requires fairly high collector breakdown voltage BV_{CE} and maximum collector current $I_{C\,\max}$ ratings which are difficult parameters to meet for a high-speed switching transistor. However, by paralleling two transistors, an adequate $I_{C\,\max}$ rating was obtained. Also, by proper selection, transistors having similar current gain β and sufficient BV_{CE} rating were obtained for the parallel pair. The average power dissipation is low because of the short time spent in the active region and because of the low values of grounded-emitter saturation voltage $V_{CE(\mathrm{sat})}$ and collector leakage current I_{CO} . For a continuous train of input pulses at a 300-megabaud rate, the average power dissipation is approximately 20 mW in each transistor.

Improvement in the speed of the output pulse amplifier was accomplished by peaking the base current with an RC network in the

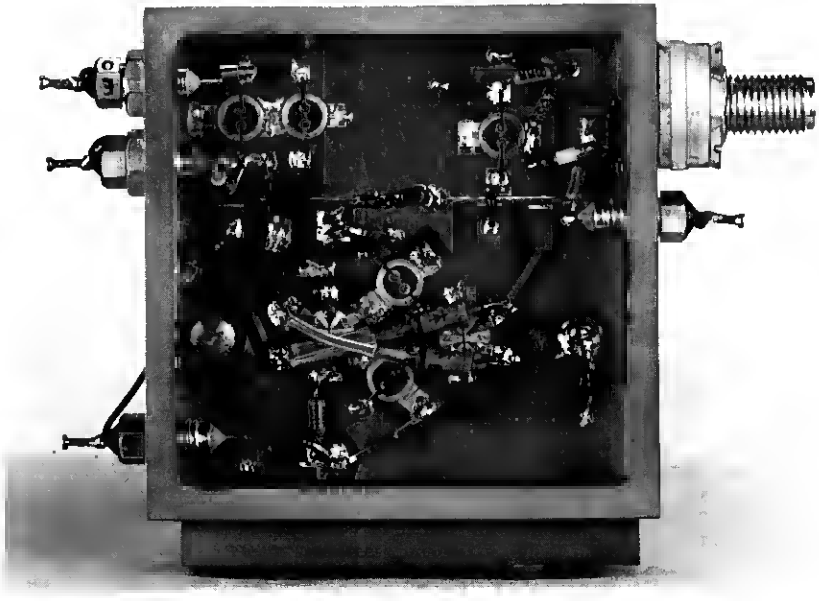

Fig. 19—A photograph of the driver.

base circuit. Reasonably close starting values for R_b and C_b were calculated by the standard formula.[25] These values were then adjusted experimentally to obtain the optimum waveshape. Typical values for R_b and C_b are 360 Ω and 100 pF. This provides an output waveform with rise and fall times of less than 1 ns and a voltage swing of 10 volts.

These circuits were constructed on epoxy glass printed circuit boards and mounted on a brass frame. Standard discrete high-frequency components are used. A photograph of the complete driver is shown in Fig. 19. A fully developed version of the driver would use hybrid integrated circuit techniques.

6.2 *Experimental Results*

In order to measure the speed of RF switching, the driver is connected to the PIN diode which is used as a transmission on-off switch. A typical result is shown in Fig. 20. RF switching times from the reverse to forward state and forward to reverse state are approximately 0.5 ns.

The amplitude characteristic of the 180-degree phase switch can be checked by monitoring the mm-wave output directly with a crystal detector. Figure 21 shows such a detector output. This indicates that the imbalance of the insertion losses in the two switching states is less than 0.2 dB. Further testing of the PLS-DCPSK modulator is done using a differential phase detector which compares the RF phases one time interval apart. The block diagram of this equipment is shown in Fig. 22 and a photograph in Fig. 23. The input signal to the differential phase detector is split by hybrid No. 1 and in one branch the delay line stores a pulse for one time interval (3.33 ns for 300-megabaud signals). The output hybrid No. 2 compares the phase of this previous pulse with the following pulse as was explained in Section II.

To demonstrate that the complete path length modulator performs properly at a 300-Mb/s rate, a simple word generator was constructed using high-speed pulse circuitry. Good reproduction of the input words

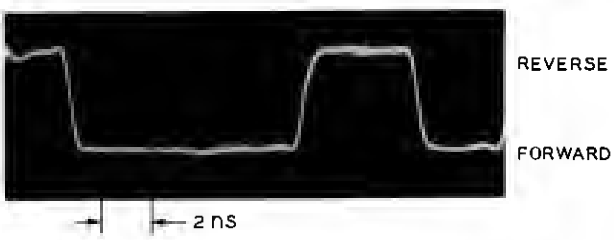

Fig. 20—Detected output of the PIN diode on-off switch.

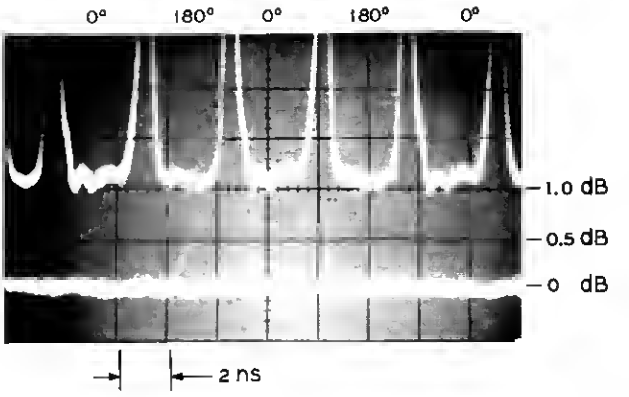

Fig. 21—Amplitude characteristic of 180-degree phase switch (circulator loss included).

was obtained at the output. The example of Fig. 24 shows the input waveform to the flip-flop circuit and the output waveform from the phase detector, corresponding to the pattern 000111000111 · · · . The average power consumption of the driver is about 0.8 W.

Table III summarizes the characteristics of the path length modulators that have been built.

VII. CONCLUSION

Considering the various factors involved in the design of mm-wave solid-state repeater systems, including the present state of device technology, the path length modulator has been proposed as one of

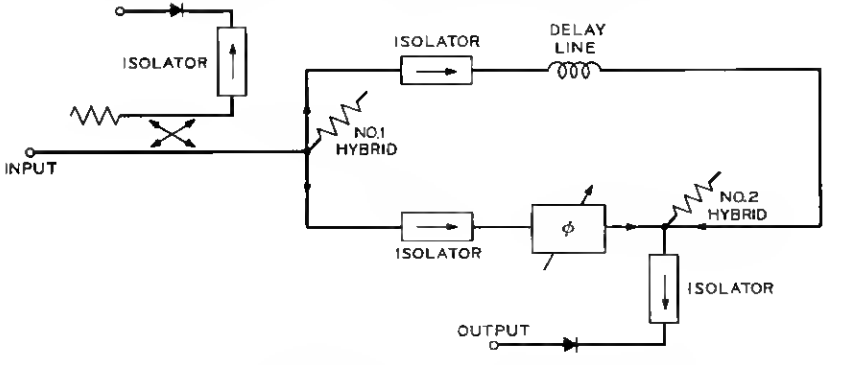

Fig. 22—A block diagram of the mm-wave phase detector.

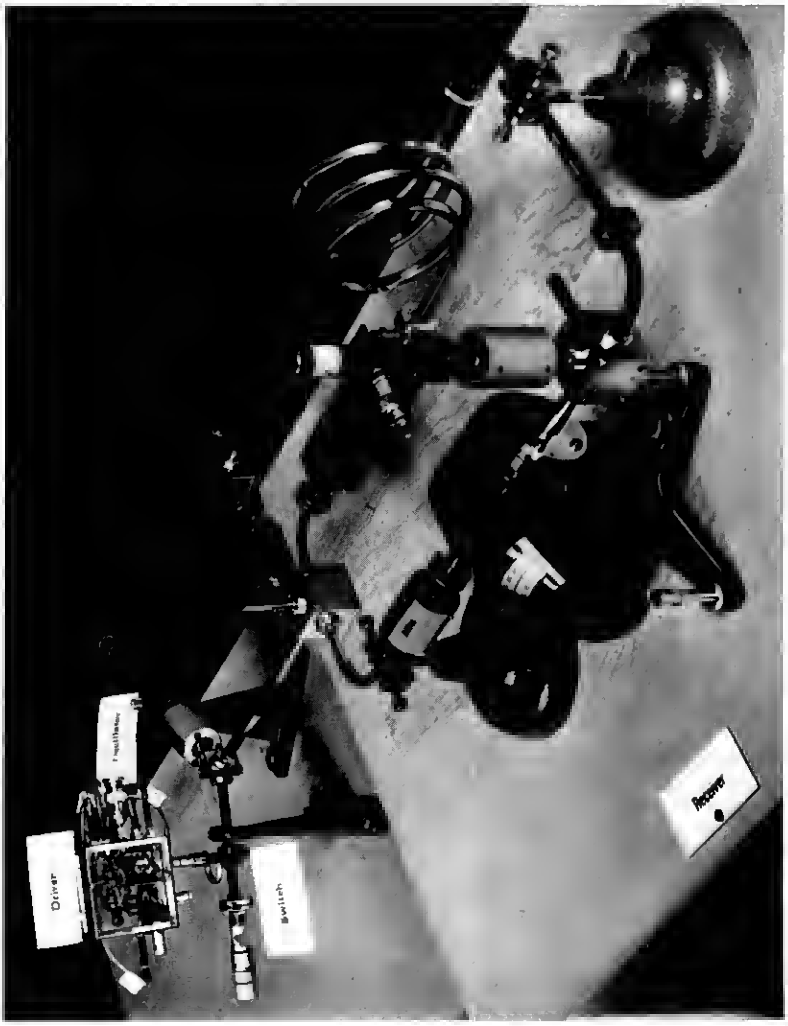

Fig. 23—A photograph of the mm-wave phase detector with Model I.

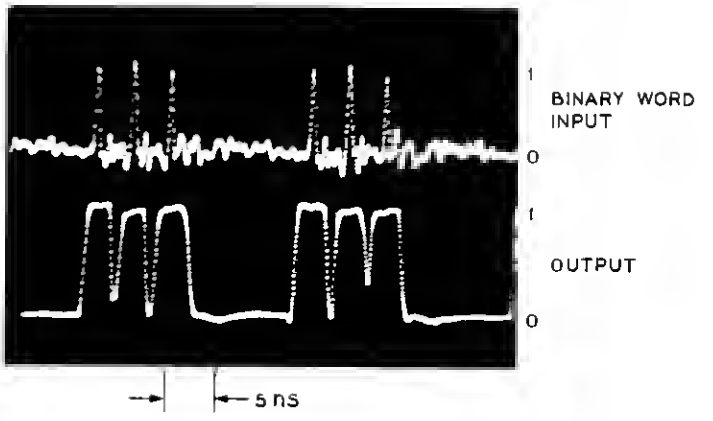

Fig. 24—Input and detected output waveform of the path length modulator.

the most promising practical modulation schemes in the mm-wave range. To demonstrate the feasibility of this proposal, three models, each consisting of an IMPATT oscillator, circulator, PIN diode switch, and its driver circuit were built. The experimental results show that the path length modulator can handle signals at 300 Mb/s. The total

TABLE III—PATH LENGTH MODULATOR CHARACTERISTICS

Characteristic	Model I†	Model II	Model III
Oscillator			
Frequency	56.4 GHz	56.4 GHz	57.4 GHz
Output Power	85 mW	135 mW	138 mW
Efficiency	2.2 %	4.1%	4.2%
Temperature Coefficient	—	−250 kHz/°C	−150 kHz/°C
Isolator			
Insertion Loss‡	1.0 dB	<0.3 dB	<0.3 dB
Modulator			
Insertion Loss Switch	0.7 dB	0.5 dB	0.6 dB
Insertion Loss Circulator	0.5 dB	0.5 dB	0.5 dB
Output Power	50 mW	100 mW	100 mW
Switching Time§			
To Forward	1.7 ns	<0.8 ns	<0.8 ns
To Reverse	1.0 ns	<0.7 ns	<0.7 ns
DC Power	0.8 W	0.8 W	0.8 W

† An early developmental model to demonstrate feasibility.
‡ A circulator with its one port terminated is used as the isolator in Model II and in Model III. For Model III, this circulator and the circulator in the modulator are integrated to form a four-port circulator.
§ Measured with the differentially coherent phase detector.

insertion loss of the modulator including two circulator passes is about 1 dB in the 50 ~ 60-GHz range, and 100 mW of output power is obtained at the output port of the circulator.

VIII. ACKNOWLEDGMENTS

Acknowledgments are due to R. Edwards who supplied the IMPATT diodes; W. Bleickardt who made the high-speed flip-flop circuit design available to us; R. E. Fisher, F. M. Magalhaes, and H. W. Thim who contributed to the initial phase of this project; and J. P. Beccone, E. E. Becker, and R. S. Riggs who assisted in the experiments. The authors wish to thank C. Barnes, F. H. Blecher, R. S. Engelbrecht, L. Moose, and K. M. Poole for their support and encouragement.

APPENDIX

An Equivalent Circuit of a PIN Diode Switch

In this appendix, we discuss the transformation necessary to get 180 degrees phase shift by a PIN diode. Suppose that the waveguide impedance is R_0 and a reciprocal two-port network is inserted between R_0 and the diode as illustrated in Fig. 25. Let the impedance looking into the two-port from the diode position be Z_a^* and define power waves at ports 1 and 2 with reference impedances R_0 and Z_a respectively. For example, the incident and reflected power waves at port 2 are given by[26]

$$a_2 = \frac{V_2 + Z_a I_2}{2\sqrt{\text{Re } Z_a}}, \qquad b_2 = \frac{V_2 - Z_a^* I_2}{2\sqrt{\text{Re } Z_a}}. \tag{1}$$

The two-port network is characterized by a scattering matrix as follows:

$$\begin{bmatrix} b_1 \\ b_2 \end{bmatrix} = S \begin{bmatrix} a_1 \\ a_2 \end{bmatrix} = \begin{bmatrix} 0 & s \\ s & 0 \end{bmatrix} \begin{bmatrix} a_1 \\ a_2 \end{bmatrix}. \tag{2}$$

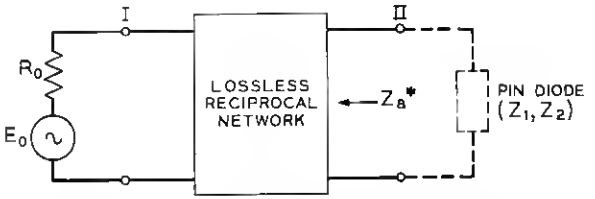

Fig. 25—Two-port network representing the switch circuit.

In the scattering matrix $S_{11} = S_{22} = 0$, since both ports are matched when the reference impedances are connected, and $S_{12} = S_{21} = s$, since reciprocity is assumed. When Z_1 is connected to port 2, $V_2 = -Z_1 I_2$. Substituting into (1), we have

$$a_2 = \frac{Z_1 - Z_a}{Z_1 + Z_a^*} b_2 . \tag{3}$$

From (2) and (3), the reflected wave at port 1 is given by

$$b_1 = sa_2 = s \frac{Z_1 - Z_a}{Z_1 + Z_a^*} b_2 = s \frac{Z_1 - Z_a}{Z_1 + Z_a^*} sa_1 .$$

Consequently, when the diode impedance is Z_1, the reflection coefficient at port 1 becomes

$$\frac{b_1}{a_1} = s^2 \frac{Z_1 - Z_a}{Z_1 + Z_a^*}.$$

Similarly, when the diode impedance is Z_2, the same reflection coefficient becomes $s^2(Z_2 - Z_a)/(Z_2 + Z_a^*)$. To get 180 degrees phase shift with equal losses in the two bias states, therefore, we have

$$\frac{Z_1 - Z_a}{Z_1 + Z_a^*} = -\frac{Z_2 - Z_a}{Z_2 + Z_a^*}. \tag{4}$$

Assuming that the denominators are not equal to zero, (4) is equivalent to

$$2Z_1Z_2 + (Z_1 + Z_2)(Z_a^* - Z_a) - 2Z_aZ_a^* = 0.$$

Suppose $Z_1 = r_1 + jx_1$, $Z_2 = r_2 + jx_2$, and $Z_a = r_a + jx_a$, then the above equation shows that

$$x_a = \frac{r_1x_2 + r_2x_1}{r_1 + r_2}, \qquad r_a = \sqrt{r_1r_2}\sqrt{1 + \frac{(x_1 - x_2)^2}{(r_1 + r_2)^2}}.$$

Figure 26 shows the equivalent circuit. If the magnitude of $x_1 = -1/\omega C$ is much larger than $|x_2|$ and r_1 and r_2 are small quantities of the same order of magnitude, we have

$$x_a \cong \frac{x_1}{1 + \frac{r_1}{r_2}}, \qquad r_a \cong \frac{|x_1|}{\sqrt{\left(1 + \frac{r_1}{r_2}\right)\left(1 + \frac{r_2}{r_1}\right)}}. \tag{5}$$

Since the exchangeable power is invariant to lossless transformations, if the two-port is lossless, the incident power P_i at port 1 in Fig. 25 can be calculated from the equivalent circuit in Fig. 26. Under the

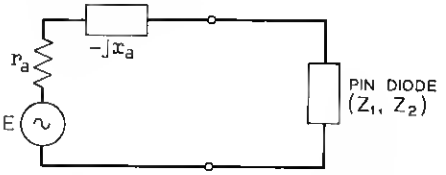

Fig. 26—Equivalent circuit of the PIN diode switch.

same approximation as (5), we obtain

$$P_i = \frac{|E_o|^2}{4R_o} = \frac{|E|^2}{4r_a} \cong \frac{|E_p|^2}{8|x_1|}\sqrt{r_1 r_2} \tag{6}$$

where E_p is the peak RF voltage applied to the diode. Equation (6) gives the maximum power handling capability of the 180-degree phase switch when E_p is limited. It is worth noting that (6) is quite different from the formula derived by M. E. Hines[27] without taking into account the insertion loss condition in the two switching states.

When E_p is equal to 10 V and $|x_1|$ is 100 Ω and $r_1 = r_2$,

$$x_a \cong -50\ \Omega, \quad r_a \cong 50\ \Omega, \quad P_i \cong -125\ \text{mW}.$$

These numbers are used in the design of the PIN diode.

REFERENCES

1. Misawa, T., "CW Millimeter-Wave IMPATT Diodes with Nearly Abrupt Junction," Proc. IEEE, *56*, No. 2 (February 1968), pp. 234–235.
2. Harkless, E. T., and Vincent, R., "A Solid-State Modulator for Millimeter Waves," ISSCC Digest of Technical Papers (1960), pp. 44–45.
3. Hubbard, W. M., and Mandeville, D. G., "Experimental Verification of the Error-Rate Performance of Two Types of Regenerative Repeaters for Differentially Coherent Phase-Shifted Keyed Signals," B.S.T.J., *46*, No. 6 (July 1967), pp. 1173–1202.
4. Hubbard, W. M., Goell, J. E., Warters, W. D., Mandeville, G. D., Lee, T. P., Shaw, R. C., and Clouser, P. L., "A Soild State Regenerative Repeater for Guided Millimeter Wave Communication Systems," B.S.T.J., *46*, No. 9 (November 1967), pp. 1977–2018.
5. Lee, T. P., Standley, R. D., and Misawa, T., "A 50 GHz Silicon IMPATT-Diode Oscillator and Amplifier," IEEE Trans. Elec. Devices., *ED-15*, No. 10 (October 1968), pp. 741–747.
6. Lee, T. P., and Standley, R. D., "Frequency Modulation of a Millimeter-Wave IMPATT Diode Oscillator and Related Harmonic Generator Effects," B.S.T.J., *48*, No. 1 (January 1969), pp. 143–161.
7. Brenner, H. E., "FM Modulation of mm-Wave IMPATT Oscillators with PCM Baseband Pulses," Proc. IEEE, *57*, No. 9 (September 1969), pp. 1683–1684.
8. Hubbard, W. M., Mandeville, G. D., and Goell, J. E., "Multilevel Modulation Techniques for Millimeter Guided Waves," B.S.T.J., *49*, No. 1 (January 1970), pp. 33–54.
9. Miyauchi, K., Kita, S., Shimada, S., and Sushi, N., "Design and Performance of an Experimental 400 MB-4PSK Guided Millimeter-Wave Transmission System," Electrical Communication Laboratory Report, NTT, Japan, 1970.

10. Nakamura, S., and Inoue, Y., "Digital 4-Phase Modulation Using Diode Switches in 2 GC Band," J. IECE, *50*, No. 6 (June 1967), pp. 127–134.
11. Murotani, M., and Tachikawa, K., "Microwave PCM System," Japan Telecommun. Rev., *9*, (November 3, 1967), pp. 126–136.
12. Kurokawa, K., "Some Basic Characteristics of Broadband Negative Resistance Oscillator Circuits," B.S.T.J., *48*, No. 6 (July–August 1969), pp. 1937–1955.
13. Pulfer, J. K., "Voltage Tuning in Tunnel Diode Oscillators," Proc. IRE, *48*, No. 6 (June 1960), p. 1155.
14. Magalhaes, F. M., and Kurokawa, K., "A Single-Tuned Oscillator for IMPATT Characterization," Proc. IEEE, *58*, No. 5 (May 1970), pp. 831–832.
15. Kenyon, N. D., "A Circuit Design for MM-Wave IMPATT Oscillators," G-MTT Symposium Digest (1970), pp. 300–303.
16. Private communication from P. T. Hutchison.
17. Kurokawa, K., *An Introduction to the Theory of Microwave Circuits*, New York: Academic Press, 1969, pp. 247–253.
18. Owen, B., and Barnes, C. E., "The Compact Turnstile Circulator," G-MTT Symposium Digest (1970), pp. 388–392.
19. Sugimoto, S.; and Sugiura, T., "Microwave Switching with Gunn-Effect Diodes," Proc. IEEE, *56*, No. 3 (March 1968), p. 371.
20. Sterzer, F., "Amplitude Modulation of Microwave Signals Using Transferred Electron Diodes," Proc. IEEE, *57*, No. 1 (January 1969), pp. 86–87.
21. Schlosser, W. O., Beccone, J. P., and Riggs, R. S., "A PIN Diode for MM-Wave Digital Modulation," G-MTT Symposium Digest (1970), pp. 114–117.
22. White, J. F., "Review of Semiconductor Microwave Phase Shifters," Proc. IEEE, *56*, No. 11 (November 1968), pp. 1924–1931.
23. Kurokawa, K., and Schlosser, W. O., "Quality Factor of Switching Diodes for Digital Modulation," Proc. IEEE, *58*, No. 1 (January 1970), pp. 180–181.
24. Koehler, D., "Semiconductor Switching at High Pulse Rates," IEEE Spectrum, *12*, No. 11 (November 1965), pp. 50–66.
25. Cillie, A. C., *Pulse and Logic Circuits*, New York: McGraw-Hill, 1968, Section 9.7.
26. Reference 17, pp. 33–38 and pp. 211–224.
27. Hines, M. E., "Fundamental Limitations in RF Switching and Phase Shifting Using Semiconductor Diodes," Proc. IEEE, *52*, No. 6 (June 1964), pp. 697–708.